

Effects of disorder on the microwave properties of MgB₂ polycrystalline films

G. Ghigo,^{1,2} G. A. Ummaryno,¹ R. Gerbaldo,^{1,2} L. Gozzelino,^{1,2} F. Laviano,^{1,2} and E. Mezzetti^{1,2}

¹*Department of Physics, Politecnico di Torino, C.so Duca degli Abruzzi 24, 10129 Torino, Italy*

²*Istituto Nazionale di Fisica Nucleare, Sez. Torino, via P. Giuria 1, 10125 Torino, Italy*

(Received 14 June 2006; revised manuscript received 18 September 2006; published 14 November 2006)

The role of disorder in superconducting magnesium diboride (MgB₂) polycrystalline films is investigated in the high frequency range by a coplanar microwave resonator technique. Two sources of disorder are considered, heavy-ion irradiation damage and sample ageing. Microwave measurements are analyzed in the framework of the two-gap model with strong interband scattering contribution. It turns out that disorder enhancement increases the interband scattering rate, resulting in a reduction of the surface resistance at low temperatures, due to a slight increase of the π gap. Moreover, increasing disorder at grain boundaries induces a nonmonotonic residual surface resistance, showing the features of a resistive behavior for the highest disorder level. Finally, the effects of the different kinds of disorder on the intrinsic and on the grain-boundary properties of the MgB₂ films are compared and discussed.

DOI: [10.1103/PhysRevB.74.184518](https://doi.org/10.1103/PhysRevB.74.184518)

PACS number(s): 74.70.Ad, 74.78.-w, 74.25.Nf, 61.80.Jh

INTRODUCTION

A comprehensive understanding of the role of disorder in two-band superconducting magnesium diboride (MgB₂) is an essential requirement for its use in potential applications. Several experiments have been carried out with samples where disorder was introduced by different methods (substitutions,¹⁻¹³ neutron and ion irradiations,¹⁴⁻²³ growth conditions²⁴). Although it is still an open issue, some points seem to be established. Disorder-induced interband scattering is expected to cause an increase of the π gap, Δ_π , and a decrease of the σ gap, Δ_σ , as well as a decrease of the critical temperature.²⁵ In fact, data reported by several groups using different characterization techniques on various types of disordered samples seem to fall onto two universal curves for Δ_π and Δ_σ , if plotted as a function of the sample's critical temperature.²⁴ Data are consistent with this picture at least down to about $T_c=25$ K, where the Δ_π enhancement is more evident. Experimental observations below 25 K are more ambiguous, and the model should include also the effects of reduced density of states.¹⁰

In this framework, the possibility to change the disorder level in the same sample, e.g., by means of ion irradiation, is of primary importance. Several experiments have been performed¹⁴⁻²³ and the overall picture that emerges is that irradiations with different particles and energies yield different results on the superconducting properties of MgB₂. Nevertheless, a common feature is that damage levels of 10^{-4} – 10^{-2} displacements per atom (d.p.a.) induced both by charged particles²² and by fast neutrons¹⁴ start to seriously degrade T_c and zero-field critical current density. For what concerns heavy ions, no clear evidence of formation of columnar defects has been reported for MgB₂,¹⁵⁻²⁰ even if flux pinning improvements have been proved, and the suppression in T_c is much less compared to high- T_c cuprates. As a further source of disorder, sample ageing has to be considered. Ageing is recognized to cause noteworthy effects, such as critical current density enhancements,²⁶ that could be attributed to the mentioned increase of the lower gap. Therefore, careful monitoring of the material response as a func-

tion of time is required, what is obviously important also from the point of view of any application. Finally, the different effect of disorder on the intrinsic and on the grain boundary properties in the case of polycrystalline films has to be distinguished, and the influence of substrate modifications, e.g., due to ion implantation in the case of irradiation, has to be taken into account.

Microwave techniques provide good probes of disorder in such systems since they offer advantages in determining the effects of small changes in the gap values. In fact, resonant microwave methods allow high-precision determination of surface resistance, R_s , and penetration depth, λ , and both of them depend exponentially on the gap. In a previous work²⁷ we showed evidence that in the low-temperature range the microwave surface resistance is accounted for by the single smaller gap Δ_π , in accordance with other literature findings,²⁸ and that the temperature dependence of the penetration depth in MgB₂ films with strong interband scattering is accounted for by an effective gap, Δ^* , which is a suitable combination of the two gaps.^{27,29} As a consequence, since disorder acts in opposite ways on the two gaps, Δ^* is expected to change much less than Δ_π and Δ_σ with the disorder level, and the same should hold for λ .

In this paper we study the effects of disorder on the microwave properties of MgB₂ films with an initially strong interband scattering and T_c around 30 K. A consistent set of results was deduced from the microwave characterization of the films, obtained by a coplanar resonator technique.^{27,30} Disorder was progressively increased in the same sample by successive 0.25 GeV Au-ion irradiations, up to a maximum fluence of 3×10^{11} cm⁻², producing d.p.a. one order of magnitude lower than in the previously cited experiments. As a further source of disorder, sample ageing has also been considered. Microwave characterizations were performed before and after each irradiation. Since the critical temperature always remains above 25 K, we interpret our data in terms of increasing interband scattering due to increasing disorder. We calculate the two gaps Δ_π and Δ_σ , and the critical temperature as a function of the interband scattering rate $\Gamma_{\pi\sigma}$, in the framework of the two-band Eliashberg theory. Afterwards, we fit the low-temperature experimental R_s data by

the standard BCS model, taking into account the gap values previously calculated. It turns out that the exact two-gap BCS formula can be well approximated by the expression proposed by Turneure *et al.*,³¹ with the single π gap. Data show that increasing disorder decreases the low-temperature surface resistance while keeping λ almost unchanged, as expected in the framework depicted above. The free parameters of the fit allow drawing some conclusions concerning the effect of the disorder on the residual surface resistance. With this respect, we consider the presence of a grain boundary network in the polycrystalline film and the fact that junctions at the grain boundaries start degrading when disorder overcomes a given threshold. Such hypothesis is also supported by the clear evidence of weak-link switching to the resistive state after the last irradiation, obtained by high input power measurements in the nonlinear regime.

EXPERIMENTAL DETAILS

MgB₂ thin films, 110 nm thick, were deposited on (0001) sapphire substrates by a coevaporation technique followed by *in situ* annealing and linear coplanar resonators have been obtained by standard photolithographic process followed by ion milling.²⁷ By means of a Rohde-Schwarz ZVK vector network analyzer we measured the complex transmission coefficient, S_{21} (ratio of the voltage transmitted to the incident voltage), as a function of the driving frequency, f . The procedure used to extract the penetration depth $\lambda(T)$ and the surface resistance $R_s(T)$ from the resonant frequency $f_0(T)$ and the unloaded quality factor $Q_0(T)$ has been reported elsewhere.²⁷

Irradiations of the resonator took place at the XTU Tandem facility of INFN - Laboratori Nazionali di Legnaro, Italy, with 250 MeV Au ions directed perpendicular to the film surface. Ions cross the whole film thickness and implant in the substrate at a mean depth of 13 μm .³² We irradiated in sequence the same sample several times, up to partial fluences of $\Phi=0.5, 1.0, 1.5, 3.0 \times 10^{11} \text{ cm}^{-2}$. The total d.p.a. is evaluated as $6 \times 10^{-17} \cdot \Phi$, with Φ expressed in cm^{-2} .³² Microwave characterizations were performed before and after each irradiation. All measurements and irradiations were performed without removing the resonator from the package, in order to avoid any possible change in the mechanical coupling between the central strip and the microwave connectors.

RESULTS AND DISCUSSION

Resonant frequency, penetration depth, unloaded quality factor, and surface resistance, as measured before and after each irradiation, are reported in Fig. 1. No significant change in the penetration depth is observed. The slight decrease of the resonant frequency as a function of irradiation fluence, reported in the inset of the upper frame, is attributed to the increase of the dielectric constant of the substrate and therefore of the line capacitance, due to ion damage and ion implantation about 13 μm below the film surface. The quality factor (lower frame) shows clear enhancements up to about 100%, below $T=10$ K. Accordingly, surface resistance sig-

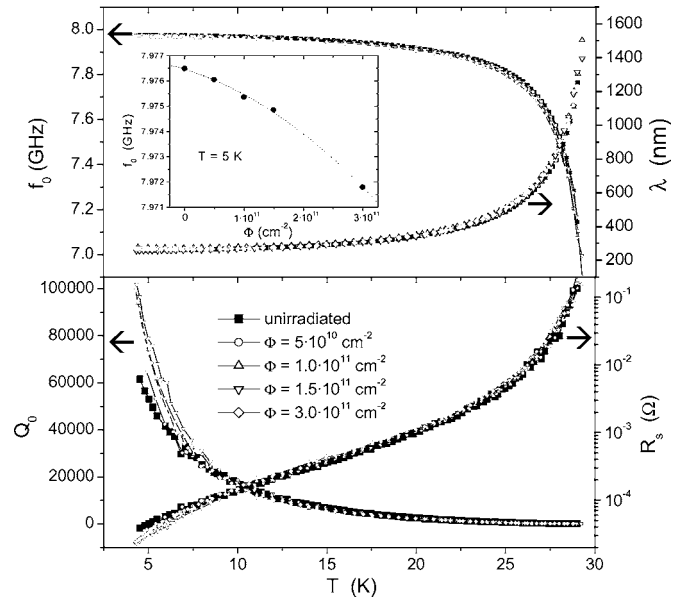


FIG. 1. Top frame: resonant frequency (left) and penetration depth (right) as a function of temperature, before and after each irradiation. The inset shows the resonant frequency at $T=5$ K as a function of irradiation fluence. Bottom frame: unloaded quality factor (left) and surface resistance (right) as a function of temperature, before and after each irradiation.

nificantly reduces at low temperatures, for the higher investigated fluences.

In order to give the correct explanation of such results we need to consider the general properties of the material and their possible evolution in the case of increasing disorder. As it is well known, MgB₂ is a two-band superconductor, with different anisotropy properties for the two bands.³³ Since we only observe a partial orientation of the c axis of the investigated films, we are not injecting rf currents in preferential direction with respect to the MgB₂ cell. Therefore, the contribution of both the bands has to be accounted for during the analysis. We accomplished this task by calculating the two gaps Δ_π and Δ_σ as a function of temperature and interband scattering rate $\Gamma_{\pi\sigma}$, in the framework of the two-band Eliashberg theory, as follows. The critical temperature of an ideal impurity-free film is fixed by a suitable μ value (prefactor of the Coulomb pseudopotential).³⁴ The effect of impurities is then added by setting the interband scattering rate $\Gamma_{\pi\sigma}$ to values that reproduce the experimental critical temperatures. We assume the spectral functions and the electron-phonon coupling constants reported in Ref. 35, the Coulomb pseudopotential as in Ref. 34, with a cutoff energy of 700 meV, and the solution calculated until a maximum energy of 800 meV. The considered densities of states at the Fermi level are 0.3 and 0.4 states/(eV unit cell) in the σ and π band, respectively. The inset of Fig. 2 shows Δ_π and Δ_σ as a function of temperature, for $\Gamma_{\pi\sigma}=0.82$, representing the case of the unirradiated resonator.²⁷ The expected increase of the π gap and decrease of the σ gap, due to disorder-induced interband scattering enhancement, are shown in Fig. 2. Also the T_c decrease as a function of $\Gamma_{\pi\sigma}$ can be calculated and it is shown in Fig. 3, together with the experimental critical tem-

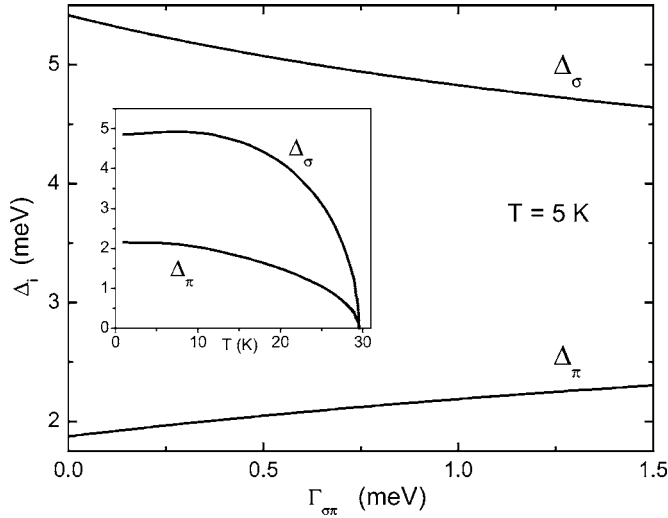


FIG. 2. Calculated σ and π gaps as a function of interband scattering rate, at $T=5$ K. In the inset, the calculated gaps are plotted as a function of temperature in the case $\Gamma_{\pi\sigma}=0.82$ meV, representing the unirradiated resonator.

peratures of the resonator under test after each irradiation. The latter have been obtained by a $f_0(T)$ fit,²⁷ and corresponding errors have been extracted from the covariance matrix of the fit parameters, evaluated from the second derivative of χ^2 at its minimum (Table I). Curves in Figs. 2 and 3 allow determining $\Gamma_{\pi\sigma}$, Δ_π , and Δ_σ from the T_c values corresponding to each irradiation (Table I). The resulting errors, as determined in the framework of the adopted model calculations, are low enough to discriminate among gap values corresponding to the different irradiation fluences. It turns out that the increase of disorder slightly enhances $\Delta_\pi(0)$. This behavior establishes a first qualitative agreement between the model and the experimental results, since we observed a corresponding reduction of R_s . In order to achieve also a quantitative agreement and to get further insight into the issue, we should consider the two-band BCS model for the surface resistance. By extending the expression proposed by Turneaure *et al.*³¹ to the two-band case, we get³⁶

$$R_s \propto \hbar \omega \sum_{i,j=1}^2 A_{ij} \int d\mathbf{q} d\mathbf{p}_{in} d\mathbf{p}_{fin} |M_{ij}|^2 N_i(0) N_j(0) I_{ij}, \quad (1)$$

where

TABLE I. Summary of the critical temperatures T_c , interband scattering rates $\Gamma_{\pi\sigma}$, gap values Δ_π and Δ_σ , fitting parameters A and R_{res} [see Eq. (3)] for the same resonator before and after Au-ion irradiation with fluence Φ .

Φ (cm ⁻²)	0	0.5×10^{11}	1.0×10^{11}	1.5×10^{11}	3.0×10^{11}
T_c (K)	29.60 ± 0.02	29.52 ± 0.02	29.46 ± 0.02	29.40 ± 0.02	29.20 ± 0.02
$\Gamma_{\sigma\pi}$ (meV)	0.82 ± 0.01	0.85 ± 0.01	0.88 ± 0.01	0.91 ± 0.01	1.02 ± 0.01
$\Delta_\pi(0)$ (meV)	2.153 ± 0.003	2.162 ± 0.003	2.170 ± 0.003	2.179 ± 0.003	2.207 ± 0.003
$\Delta_\sigma(0)$ (meV)	4.848 ± 0.004	4.834 ± 0.004	4.819 ± 0.004	4.805 ± 0.004	4.755 ± 0.004
A (m Ω)	2.38 ± 0.05	2.76 ± 0.09	2.81 ± 0.09	2.73 ± 0.07	3.07 ± 0.04
R_{res} ($\mu\Omega$)	31 ± 1	25 ± 2	16 ± 2	13 ± 2	17 ± 1

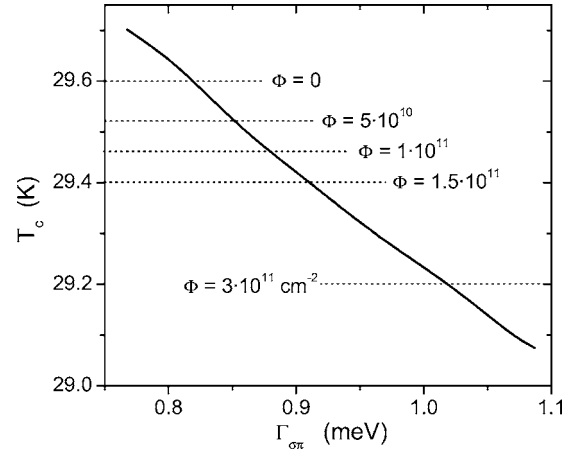


FIG. 3. Calculated decrease of the critical temperature with interband scattering rate. Critical temperatures, obtained by the fit of experimental $f_0(T)$ after each irradiation (Ref. 27), are indicated by dotted lines.

$$I_{ij} = \int_{-\infty}^{+\infty} \left[\frac{|E| |E + \hbar \omega|}{\sqrt{E^2 - \Delta_i^2}} + \frac{\Delta_i}{\sqrt{E^2 - \Delta_i^2}} \operatorname{sgn}(E) \frac{\Delta_j \operatorname{sgn}(E + \hbar \omega)}{\sqrt{(E + \hbar \omega)^2 - \Delta_j^2}} \right] \times [F(E) - F(E + \hbar \omega)] dE,$$

$\hbar \omega$ is the energy of the absorbed photon, \mathbf{p}_{in} , \mathbf{p}_{fin} are the quasiparticles momenta, \mathbf{q} is the photon momentum, the matrix $|M(\mathbf{p}_{in}, \mathbf{p}_{fin}, \mathbf{q}, \hbar \omega)|$ is integrated over available quasiparticles and photons states, F is the Fermi function, Δ_i is the gap of i band, $N_i(0)$ is the density of states at the Fermi level of i band and A_{ij} are the corresponding weights. The inset of Fig. 4 shows the comparison between the curve obtained by the exact two-gap formula (1) with realistic weights for the two gaps (curve no. 1), the curve obtained from (1) by neglecting the σ -band contribution (curve no. 2) and its approximation for $T < T_c/2$, $\hbar \omega \ll k_B T$, and $\hbar \omega \ll \Delta$ (curve no. 3)

$$R_s \propto \frac{(\hbar \omega)^2}{k_B T} \ln \left(\frac{4k_B T}{\hbar \omega} \right) \exp \left(-\frac{\Delta_\pi(T)}{k_B T} \right) \quad (2)$$

that matches the expression given in Ref. 31, with $\Delta = \Delta_\pi$.³⁷ The good agreement among the three curves for $T < 10$ K

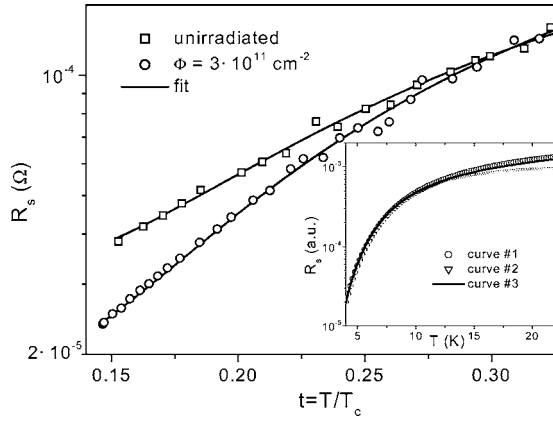


FIG. 4. Main frame: fit of the low temperature R_s data by (3), in the case of the sample before irradiation and after the highest-dose irradiation. Inset: comparison between the surface resistance calculated by the exact two-gap formula (1) with realistic weights for the two gaps ($A_\pi=0.6$, $A_\sigma=0.3$, $A_{\sigma\pi}=A_{\pi\sigma}=0.05$, curve no. 1, circles), the curve obtained from (1) by neglecting the σ -band contribution (curve no. 2, triangles) and its analytical approximation (curve no. 3, solid line) for $T < T_c/2$, $\hbar\omega \ll k_B T$, and $\hbar\omega \ll \Delta$.

allows us to fit the experimental data by the analytical expression (2), rewritten as

$$R_s(T) = \frac{A}{T} \ln\left(\frac{4k_B T}{\hbar\omega}\right) \exp\left(-\frac{\Delta_\pi(T)}{k_B T}\right) + R_{res}, \quad (3)$$

where A is a constant and a temperature independent residual resistance term R_{res} has been added. R_{res} represents the dissipative contribution of the fraction of unpaired electrons at low temperature. Results concerning fitting of data before irradiation and after the highest-dose irradiation are shown in Fig. 4 and the two free parameters A and R_{res} are reported in Table I for each irradiation. In Fig. 5 the residual resistance is plotted as a function of the interband scattering rate and exhibits a minimum in correspondence to about $\Gamma_{\pi\sigma} = 0.95$ meV.

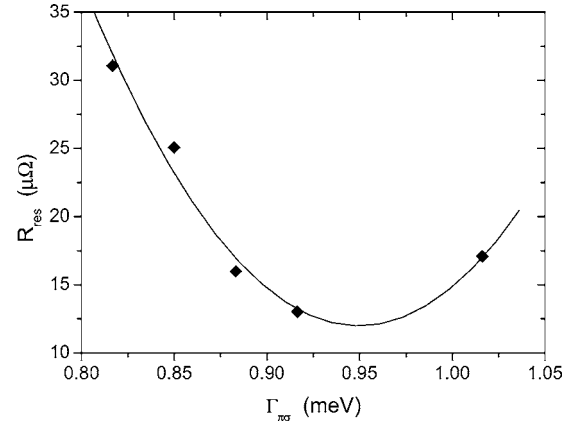


FIG. 5. Behavior of the fitting parameter R_{res} (surface residual resistance) as a function of the interband scattering rate (the line is a guide for eye).

In order to explain the nonmonotonic R_{res} behavior, the presence of grain boundaries acting as Josephson junctions in the polycrystalline film is considered. Such junctions in MgB_2 films are known to be of high-conductivity SNS type.³⁸ Nevertheless, we clearly observe a transition to a SIS-type weak-link behavior in measurements as a function of input power. Figures 6(a) and 6(b) show the typical deformations of the resonance curve due to nonlinear effects, as the input power is increased. In Fig. 6(c), which represent the case of highest disorder here considered, evidence of weak-link switch to resistive behavior is pointed out by the vertical “steps” in the resonance curves.³⁹ In previous measurements such weak links could be also present, but they were under critical. As a further element of the discussion, we remind one that in this case the surface residual resistance $R_{res} \propto j_{cJ}^{-3/2} R_{bl}^{-1}$, where j_{cJ} is the junction critical current density and R_{bl} is the normal leakage current resistance.⁴⁰ Once established the existence of these mechanisms, the presence of the R_{res} minimum reasonably follows as the balance between two competing effects, both caused by disorder, namely enhancement of R_{bl} and decrease of j_{cJ} . We argue that the ini-

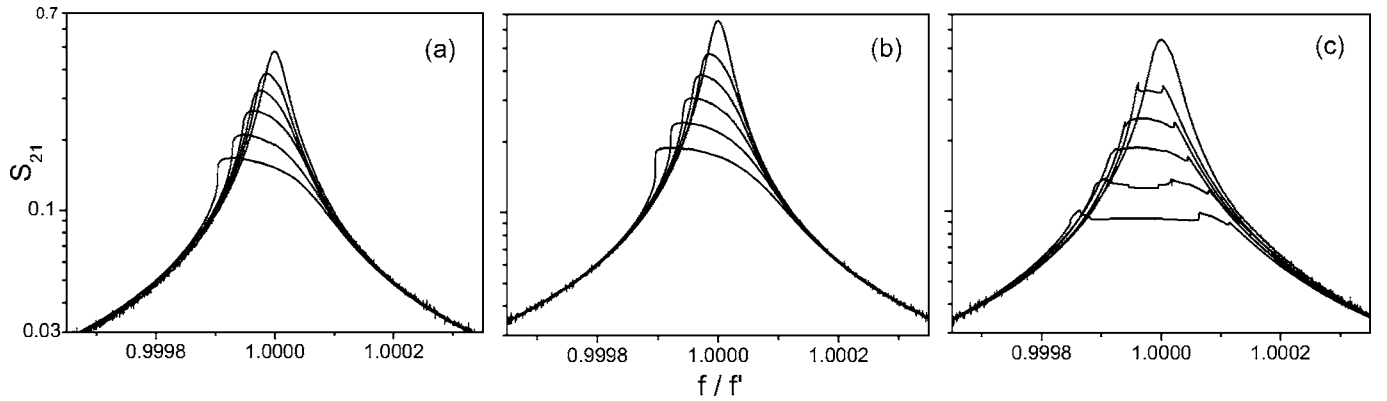


FIG. 6. Experimental resonance curves of the same resonator at three different levels of disorder [$\Gamma_{\pi\sigma}=0.82$, 0.91 , and 1.02 meV for (a), (b) and (c), respectively]. In each panel, several curves are shown for different input power levels (-20 , -7 , -4 , -1 , 2 , and 5 dBm). The normalization factor f' is the resonant frequency of the lower input-power curve. Nonlinearity effects cause the progressive distortion of the curves at increasing input power. Curves of figure (c) show also the typical features of weak-link switching to resistive state (downward steps in the ascending part of the curve and upward steps in the descending part).

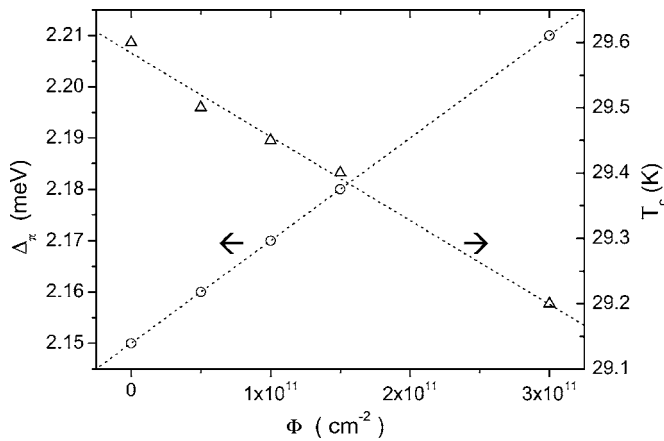


FIG. 7. Critical temperature (right) and π gap (left) as a function of irradiation fluence.

tial decrease of R_{res} as a function of disorder level is due to higher sensitivity to R_{bl} variations. The ensuing R_{res} increase marks the emerging of the j_{cJ} -dependent term, that finally starts to critically degrade the junctions.

Finally, we comment on the possibility to distinguish the influence of different kinds of disorder on the intrinsic and on the grain-boundary properties of the polycrystalline film. Although no ultimate distinction is in principle possible, hints suggesting how irradiation-induced and age-induced disorder operates can be found. For what concerns the intrinsic intragrain properties, the linear correlation between π gap or T_c and irradiation fluence (Fig. 7) clearly suggests a role of heavy-ion induced defects. On the other hand, grain-boundary modifications, mirrored by the behavior of the residual surface resistance, seem to be mainly ruled by ageing. In Fig. 8 the inverse of the unloaded quality factor at $T = 5$ K, proportional to the residual surface resistance, is reported as a function of sample age. Solid symbols represent measurements on the unirradiated resonator, while open symbols represent measurements after irradiations up to the indicated fluence. The initial decrease shown by unirradiated-sample data and the final increase shown by the last two points, measured just after the last irradiation and two months later, suggest that the R_{res} minimum is age induced. At higher temperatures this effect is smeared out (data at $T = 10$ K are reported).

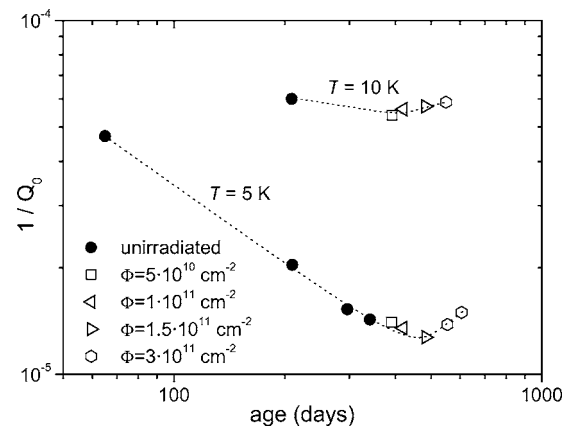


FIG. 8. Inverse of the unloaded quality factor at $T = 5$ and 10 K, as a function of the sample age. Each solid symbol represents the average of several measurements on the unirradiated resonator, while open symbols represent measurements after irradiation up to the indicated fluence. Dotted lines are guides for eye.

In summary, microwave characterization of MgB_2 thin films as a function of heavy-ion irradiation and ageing-induced disorder has been presented in the framework of the two-gap model with interband scattering contribution. Enhanced disorder results in a remarkable reduction of the surface resistance at low temperature, due to a slightly-increased Δ_π and to disorder effects on weak links, inducing a non-monotonic residual resistance. Data seem to indicate that irradiation-induced disorder plays a role in modifying the intrinsic properties of the material and age-induced disorder determines the grain-boundary properties of such polycrystalline films, even though overlaying effects are not to be excluded. These results extend to the high frequency domain the picture already established by other experimental techniques, concerning the role of disorder in two-band superconducting MgB_2 , and could be useful for material engineering aimed at microwave applications.

ACKNOWLEDGMENTS

The authors wish to thank D. Andreone and B. Minetti for fruitful discussions, and E. Monticone for sample preparation. This work has been partially supported by INFN under the project DiSCoLI and by the Italian MIUR under the project FIRB-RBAU01PEMR.

- ¹J. Y. Xiang, D. N. Zheng, J. Q. Li, L. Li, P. L. Lang, H. Chen, C. Dong, G. C. Che, Z. A. Ren, H. H. Qi, H. Y. Tian, Y. M. Ni, and Z. M. Zhao, Phys. Rev. B **65**, 214536 (2002).
- ²P. Postorino, A. Congeduti, P. Dore, A. Nucara, A. Bianconi, D. Di Castro, S. De Negri, and A. Saccone, Phys. Rev. B **65**, 020507 (2001).
- ³G. Papavassiliou, M. Pissas, M. Karayanni, M. Fardis, S. Koutandos, and K. Prassides, Phys. Rev. B **66**, 140514(R) (2002).
- ⁴A. Bianconi, S. Agrestini, D. Di Castro, G. Campi, G. Zangari, N. L. Saini, A. Saccone, S. De Negri, M. Giovannini, G. Profeta, A. Continenza, G. Satta, S. Massidda, A. Cassetta, A. Pifferi, and

M. Colapietro, Phys. Rev. B **65**, 174515 (2002).

- ⁵O. de la Pena, A. Aguayo, and R. de Coss, Phys. Rev. B **66**, 012511 (2002).
- ⁶M. Putti, M. Affronte, P. Manfrinetti, and A. Palenzona, Phys. Rev. B **68**, 094514 (2003).
- ⁷R. A. Ribeiro, S. L. Bud'ko, C. Petrovic, and P. C. Canfield, Physica C **384**, 227 (2003).
- ⁸H. Schmidt, K. E. Gray, D. G. Hinks, J. F. Zasadzinski, M. Avdeev, J. D. Jorgensen, and J. C. Burley, Phys. Rev. B **68**, 060508(R) (2003).
- ⁹K. Papagelis, J. Arvanitidis, K. Prassides, A. Schenck, T. Taken-

- bou, and Y. Iwasa, *Europhys. Lett.* **61**, 254 (2003).
- ¹⁰J. Kortus, O. V. Dolgov, R. K. Kremer, and A. A. Golubov, *Phys. Rev. Lett.* **94**, 027002 (2005).
- ¹¹S. Slusky, N. Rogado, K. A. Regan, M. A. Hayward, P. Khalifah, T. He, K. Inumaru, S. M. Loureiro, M. K. Haas, H. W. Zandbergen, and R. J. Cava, *Nature (London)* **410**, 343 (2001).
- ¹²D. Di Castro, S. Agrestini, G. Campi, A. Cassetta, M. Colapietro, A. Congeduti, A. Continenza, S. De Negri, M. Giovannini, S. Massidda, M. Nardone, A. Pifferi, P. Postorino, G. Profeta, A. Saccone, N. L. Saini, G. Satta, and A. Bianconi, *Europhys. Lett.* **58**, 278 (2002).
- ¹³V. Likodimos, S. Koutandos, M. Pissas, G. Papavassiliou, and K. Prassides, *Europhys. Lett.* **61**, 116 (2003).
- ¹⁴Y. Wang, F. Bouquet, I. Sheikin, P. Toulemonde, B. Revaz, M. Eisterer, H. W. Weber, J. Hinderer, and A. Junod, *J. Phys.: Condens. Matter* **15**, 883 (2003).
- ¹⁵S. R. Shinde, S. B. Ogale, J. Higgins, R. J. Choudhary, V. N. Kulkarni, H. Zheng, R. Ramesh, A. V. Pogrebnyakov, S. Y. Xu, Q. Li, X. X. Xi, J. M. Redwing, and D. Kanjilal, *Appl. Phys. Lett.* **84**, 2352 (2004).
- ¹⁶R. Olsson, W. Kwok, G. Karapetrov, M. Iavarone, H. Claus, C. Peterson, G. W. Carlbtree, W. N. Kang, H. J. Kim, E. M. Choi, and Sung-Ik Lee, *cond-mat/0201022* (unpublished).
- ¹⁷N. Chikumoto, A. Yamamoto, M. Konczykowski, and M. Murakami, *Physica C* **378-381**, 466 (2002).
- ¹⁸S. Okayasu, M. Sasase, K. Hojou, Y. Chimi, A. Iwase, H. Ikeda, R. Yoshizaki, T. Kambara, H. Sato, Y. Hamatani, and A. Maeda, *Physica C* **382**, 104 (2002).
- ¹⁹M. Putti, V. Braccini, C. Ferdeghini, F. Gatti, G. Grasso, P. Manfrinetti, D. Marrè, A. Palenzona, I. Pallecchi, C. Tarantini, I. Sheikin, H. U. Aebersold, and E. Lehmann, *Appl. Phys. Lett.* **86**, 112503 (2005).
- ²⁰R. Gandikota, R. K. Singh, J. Kim, B. Wilkens, N. Newman, J. M. Rowell, A. V. Pogrebnyakov, X. X. Xi, M. M. Redwing, S. Y. Xu, and Q. Li, *Appl. Phys. Lett.* **86**, 012508 (2005).
- ²¹R. H. T. Wilke, S. L. Bud'ko, P. C. Canfield, J. Famer, and S. T. Hannahs, *Phys. Rev. B* **73**, 134512 (2006).
- ²²Y. Bogoslavsky, L. F. Cohen, G. K. Perkins, M. Polichetti, T. J. Tate, R. Gwilliam, and A. D. Caplin, *Nature (London)* **411**, 561 (2001).
- ²³S. D. Kaushik, Ravi Kumar, P. K. Mishra, J. E. Giencke, C. B. Eom, and S. Patnaik, *cond-mat/0509755* (unpublished).
- ²⁴M. Iavarone, R. Di Capua, A. E. Koshelev, W. K. Kwok, F. Chiarella, R. Vaglio, W. N. Kang, E. M. Choi, H. J. Kim, S. I. Lee, A. V. Pogrebnyakov, J. M. Redwing, and X. X. Xi, *Phys. Rev. B* **71**, 214502 (2005).
- ²⁵S. C. Erwin and I. I. Mazin, *Phys. Rev. B* **68**, 132505 (2003). demonstrated that only out-of-plane distortions in the Mg layer could lead to this effect.
- ²⁶G. K. Perkins, Y. Bugoslavsky, A. D. Caplin, J. Moore, T. J. Tate, R. Gwilliam, J. Jun, S. M. Kazakov, J. Karpinski, and L. F. Cohen, *Supercond. Sci. Technol.*, **17**, 232 (2004).
- ²⁷G. Ghigo, D. Botta, A. Chiodoni, L. Gozzelino, R. Gerbaldo, F. Laviano, E. Mezzetti, E. Monticone, and C. Portesi, *Phys. Rev. B* **71**, 214522 (2005).
- ²⁸B. B. Jin, T. Dahm, A. I. Gubin, E. M. Choi, H. J. Kim, S. I. Lee, W. N. Kang, and N. Klein, *Phys. Rev. Lett.* **91**, 127006 (2003).
- ²⁹V. G. Kogan and N. V. Zhelezina, *Phys. Lett. B* **69**, 132506 (2004).
- ³⁰G. Ghigo, D. Andreone, D. Botta, A. Chiodoni, R. Gerbaldo, L. Gozzelino, F. Laviano, B. Minetti, and E. Mezzetti, *Supercond. Sci. Technol.* **18**, 193 (2005).
- ³¹J. P. Turneaure, J. Halbritter, and H. A. Schwetman, *J. Supercond.* **4**, 341 (1991).
- ³²Calculations based on: J. Ziegler, *The Stopping and Range of Ions in Solids*, Vol. 1 (Pergamon Press, Oxford, 1985).
- ³³H. J. Choi, D. Roundy, H. Sun, M. L. Cohen, and S. G. Louie, *Nature (London)* **418**, 758 (2002).
- ³⁴G. A. Ummarino, R. S. Gonnelli, S. Massidda, and A. Bianconi, *Physica C* **407**, 121 (2004).
- ³⁵A. Brinkman, A. A. Golubov, H. Rogalla, O. V. Dolgov, J. Kortus, Y. Kong, O. Jepsen, and O. K. Andersen, *Phys. Rev. B* **65**, 180517(R) (2002).
- ³⁶S. V. Barabash and D. Stroud, *Phys. Rev. B* **66**, 172501 (2002).
- ³⁷Due to the presence of impurities and disorder, the explicit dependence of Δ_{π} on temperature has to be considered in (2) also at low temperatures, since it can significantly vary from the usual nearly constant value.
- ³⁸S. B. Samanta, H. Narayan, A. Gupta, A. V. Narlikar, T. Muranaka, and J. Akimitsu, *Phys. Rev. B* **65**, 092510 (2002).
- ³⁹J. Wosik, L. M. Xie, R. Grabovickic, T. Hogan, and S. A. Long, *IEEE Trans. Appl. Supercond.* **9**, 2456 (1999).
- ⁴⁰J. Halbritter, *Supercond. Sci. Technol.* **12**, 883 (1999).